Rheological Study of the Sol−Gel Transition of Hybrid Gels

Yue Zhao,[†] Yi Cao,[‡] Yuliang Yang,*[,‡] and Chi Wu*[,†,§]

The Opening Laboratory for Bond-selective Chemistry, Department of Chemical Physics, University of Science and Technology of China, Hefei, Anhui, China; Department of Macromolecular Science, Fudan University, The Open Laboratory of Macromolecular Engineering, State Commission of Education, Shanghai, China; and Department of Chemistry, The Chinese University of Hong Kong, Shatin, N.T., Hong Kong

Received June 13, 2002; Revised Manuscript Received November 5, 2002

ABSTRACT: As the temperature decreases, thermally sensitive spherical poly(*N*-isopropylacrylamide) (PNIPAM) microgels with a lower critical solution temperature (LCST ∼ 32 °C) swell in a dispersion, leading to a possible volume−concentration induced sol−gel transition if the microgel concentration is sufficiently high. In such a formed gel, polymer chains inside each microgel were *chemically* cross-linked, but individual microgels were *physically* close-packed into a three-dimensional network. Such hybrid gels can be used as model systems for studying the sol−gel transition, which avoids several problems, such as chain entanglements, phase separation, and vitrification, normally occurring in a gelling process. The sol−gel transition of such hybrid gels was studied by the change of viscoelastic modulus G' and G''. As expected, the sol−gel transition depends on the polymer concentration, frequency, and shear stress. The gelation point could be roughly estimated by the method of Winter and Chambon. Our results showed that the temperature dependence of G'' and tan δ ($=G''/G'$) had a minimum, which corresponded to the sol−gel transition, providing a better way to determine the sol−gel transition temperature.

Downloaded via UNIV SCIENCE AND TECHNOLOGY CHINA on May 11, 2020 at 02:31:17 (UTC).
See https://pubs.acs.org/sharingguidelines for options on how to legitimately share published articles.

Introduction

A gel is normally made of a stable chemically or physically cross-linked network swollen with a lot of solvent. As a multicomponent system, its composition is like a liquid, but it contains continuous solid and fluid phases of colloidal dimensions.[1,2] The network structure can be formed by either a chemical or a physical gelation process. In a chemical process, linear chains gradually turn into branched clusters, and then clusters are interconnected by covalent bonds to form a network structure. In a physical process, various forces, such as van der Waals, electrostatic attraction, and hydrogen bonding, can be employed to bind polymer chains together to form a gel network. Therefore, the sol−gel transition in physical gels is often reversible.[3−6] In a gelation process, the sol−gel transition point, such as a particular temperature or volume concentration, is of primary importance in characterizing the gel formation.[7−9] The sol−gel transition point can be determined by a sudden change of a range of physical properties.[10] In theory, the criterion of gel formation is the existence of one long chain running through the whole system; i.e., its molar mass becomes infinite. In practice, a sudden loss of flow is the most common and conventional test to determine the sol−gel transition point since at the gelation point the viscoelastic properties change abruptly from an initially liquidlike state to a solidlike state.[11−17] However, a precise experimental determination of the exact transition point is rather difficult because of its divergent nature. We recently showed that forced Rayleigh scattering could be used to detect the sol−gel transition of a physical gel in terms of the movement of photochromic probes on the scale of several micrometers.[18] This provides a very precise determination of the melting point. The problem is that such an optical method requires the labeling of polymer chains inside a gel network.

The formation of a chemical gel is normally irreversible, which makes the determination of the exact sol−gel transition point even more difficult, while for reversible physical gels, there often exists a hysteresis in the melting process, which also complicates the investigation of the gelation process and gel structure. Moreover, the sol−gel transition is often accompanied by vitrification, chain entanglement, and phase transition. Recently, we have adopted a hybrid hydrogel for the study of the sol−gel transition, in which billions of swollen thermally sensitive spherical poly(*N*-isopropylacrylamide) (PNIPAM) microgels are physically close-packed, as schematically shown below.

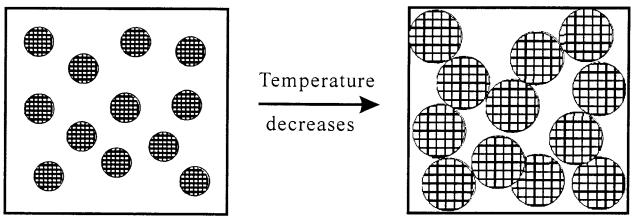

Note that inside each microgel polymer chains were *chemically* cross-linked. Therefore, this is a "hybrid" chemical/physical gel, which resembles a glass in which atoms or small molecules are replaced by much large spherical microgels (∼100 nm). The sol−gel transition of such a hybrid gel is extremely "clean" without the interference of vitrification, chain entanglement, and phase transition, normally occurring in a gelling process. The structure inhomogeneity due to chemical cross-linking is limited within individual microgels (i.e., <100 nm). As "building blocks", the microgels were narrowly distributed and well characterized. Moreover, the gelation of such a dispersion is completely thermoreversible without any hysteresis. Previously, we have studied the static nonergodicity of such a hybrid gel by

[†] University of Science and Technology of China.
[‡] Fudan University.
[§] The Chinese University of Hong Kong.

10.1021/ma020919y CCC: $25.00 © 2003 American Chemical Society
Published on Web 01/07/2003

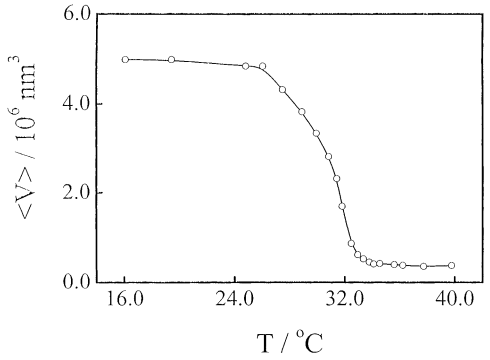

Figure 1. Temperature dependence of average hydrodynamic volume $\langle V \rangle$ of dilute microgel solution, measured from laser light scattering, where the microgel concentration is 6.06×10^{-5} g/mL.

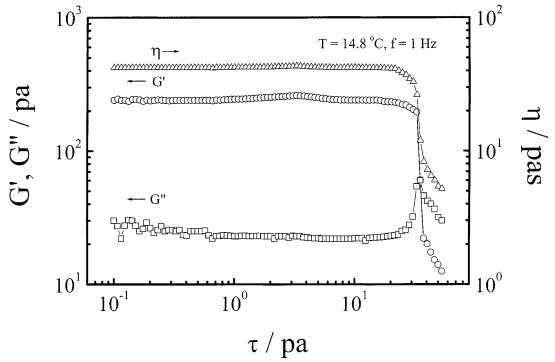

Figure 2. Stress dependence of dynamic moduli (G' and G'') and viscosity (η) of a typical hybrid gel at a temperature much lower than the gelation temperature (~28 °C), where the microgel concentrations is 4.64×10^{-2} g/mL.

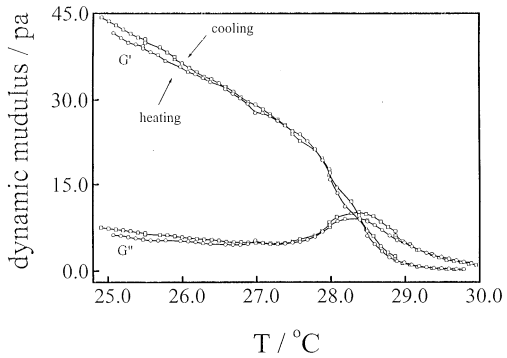

Figure 3. Temperature dependence of dynamic moduli (G' and G'') during isochronal dynamic temperature sweep experiments in the heating and cooling process, where the microgel concentrations is 4.64×10^{-2} g/mL, $\sigma = 1$ Pa, and $f = 1$ Hz.

a combination of static and dynamic laser light scattering.[19] Our results showed that the observed static nonergodicity was not intrinsic but strongly depended on how the dispersion was gelled. The present study was designed to have a better understanding of its viscoelastic property as well as its sol−gel transition process.

Experimental Section

Sample Preparation. *N*-Isopropylacrylamide (NIPAM) was recrystallized three times in a benzene/*n*-hexane mixture. *N*,*N*′-Methylenebis(acrylamide) (BIS, from Aldrich, analytical grade) as cross-linker was recrystallized from methanol. Potassium persulfate (KPS, from Aldrich, analytical grade) as initiator and anionic surfactant sodium dodecyl sulfate (SDS) as dispersant were used without further purification. 4.0 g of NIPAM, 0.076 g of BIS, and 0.076 g of SDS were dissolved into 250 mL of deionized water in a 500 mL reactor fitted with a nitrogen bubbling inlet and outlet, a magnet stirrer, and a reflux condenser. After the solution was stirred for 40 min at 70 °C under nitrogen purge, 0.155 g of KPS dissolved in 20 mL of deionized water was introduced to start the polymerization. The reaction mixture was kept at 70 °C for 8 h. The unreacted monomer and most of SDS were removed by adding the reaction mixture dropwise into 250 mL of methanol. The resulting precipitate was dissolved in 80 mL of deionized water and was reprecipitated in an equal volume of methanol. To remove the remaining trace amount of SDS and other impurities, the microgels were further purified by three cycles of successive centrifugation, decantation, and redispersion in deionized water.[20] The resultant dispersion had a ζ potential close to zero. Such purified dispersion was then concentrated to different desired concentrations.

Viscometry. A HAAKE RS75 rheometer with a cone and plate (radius 30 mm, cone angle 2°) was used to measure dynamic rheological properties of hybrid gels. The temperature was controlled by an external thermal bath, with an accuracy of ca. ±0.1 °C. At each gelation temperature, viscoelastic parameters (the elastic and viscous moduli, G' and G'') were used to monitor the gelation kinetics. To avoid any possible sample disruption during the gelation, all the parameters were measured from linear viscoelastic spectra.

Results and Discussion

Figure 1 shows a typical temperature dependence of the average hydrodynamic volume of the microgels in a dilute dispersion (6.06×10^{-5} g/mL), where $\langle V \rangle$ is defined as $4\pi\langle R_h \rangle^3/3$ and $\langle R_h \rangle$ is the average hydrodynamic radius determined by dynamic laser light scattering (LLS). Details of the LLS theory and instrumentation can be found elsewhere.[21−23] In the temperature range studied, the swelling and shrinking of individual microgels were reversible without any hysteresis. It is helpful to note that the temperature change of ~6 °C can lead to a ~13-fold volume change. In such a dilute dispersion, the microgels only occupy 0.26% of the volume of the dispersion even in the swollen state. Therefore, there is nearly no interparticle interaction in such a dilute dispersion. The ratio of the average radius of gyration $\langle R_g \rangle$ from static LLS to $\langle R_h \rangle$ is ~0.8, indicating that the microgels are uniform and spherical-like.[21] After the dispersion was concentrated ~10^3 times to 4.91×10^{-2} g/mL, the swelling of individual microgels as the temperature decreased from 32 to 25 °C could lead to a volume concentration change from 16.2% to over 100% so that the swollen microgels are packed together to form a hybrid gel, resulting in a volume−concentration induced sol−gel transition.

Figure 2 shows the stress dependence of G', G'', and viscosity η of a typical hybrid gel formed at a temperature much lower than the gelation temperature. It is clear that there is no significant change in G', G'', and η as long as the stress is less than 20 Pa. The sharp decrease of G' and η at $\tau \sim 30$ Pa can be attributed to the starting of the stress-induced sliding between the microgels, which is expected because the interaction between the microgels is the weak physical force. To avoid such a sliding, we decided to study the temperature dependence of the viscoelasticity of the hybrid gels in the stress range $1 \leq \tau \leq 3$.

Figure 3 shows the temperature dependence of G' and G'' during isochronal dynamic temperature sweeping experiments in a heating-and-cooling cycle. It shows that the rheological behavior of the hybrid gel is essentially reversible. We reached a similar conclusion in the LLS study.[19] Previous studies of various gels showed that the gelation point was located in the

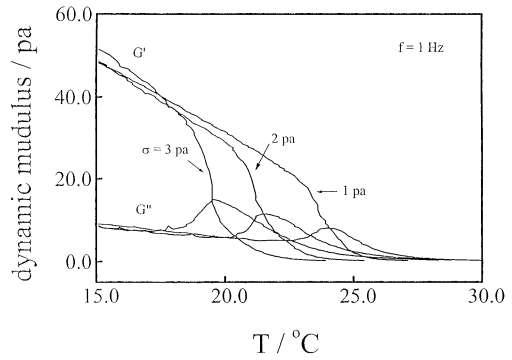

Figure 4. Temperature dependence of the dynamic moduli (G' and G'') at different shear stress amplitude, where the microgel concentration is 3.39×10^{-2} g/mL, $f = 1$ Hz, and $\sigma =$ 1, 2, and 3 Pa.

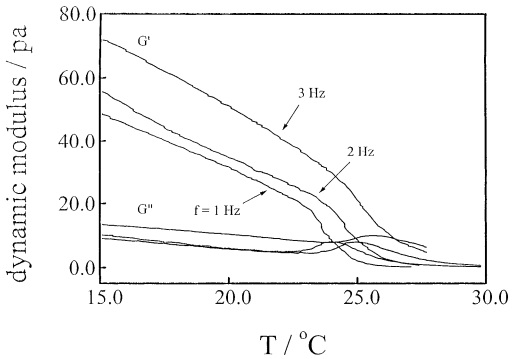

Figure 5. Temperature dependence of the dynamic moduli (G' and G'') at different frequency, where the microgel concentration is 3.39×10^{-2} g/mL, $\sigma = 1$ Pa, and $f = 1$, 2, and 3 Hz.

vicinity of the yield state, defined as the intersection between elastic (storage) modulus G' and viscous (loss) modulus G''.[24−26] On the other hand, the gelation could also be described by the evolution of loss tangent tan(δ), defined as G''/G'. This is because tan(δ) $\rightarrow \infty$ at the onset of the process (fluid behavior) and tan(δ) $\rightarrow 0$ after the gelation is complete. Winter et al.[27] showed that when the gelation point does not correspond to the intersection of G' and G'', the gelation point could be related to the critical conversion point (p_c) of a crosslinking reaction. This is because the frequency dependence of both G' and G'' is proportional to ω^n, where n is a constant.[27,28] Therefore, tan(δ) becomes independent of frequency at the gelation point and $\delta = n\pi/2$ with $0 < n < 1$. If $n \rightarrow 1$, the gel is viscous, while for $n \rightarrow 0$, the gel is elastic or rigid. It has been shown that for the gelation of poly(dimethylsiloxane) (PDMS)[27] $n = 0.5$.

Figure 4 shows that for a given shear frequency (f) the temperature dependence of G' and G'' shifts as the shear stress (σ) changes. The temperature at which G' and G'' intersect decreases as σ increases. This is reasonable because when a lower σ is applied, the structural destruction rate is relatively lower than the structural recovery rate. Figure 4 clearly shows that the effect of σ on G' and G'' mainly occurs near the gelation temperature. On the other hand, Figure 5 shows that, for a given σ, the temperature at which G' and G'' intersect decreases with f. Relatively, f has a lesser effect on the intersection temperature than σ. As expected, rheological properties of such a system are less dependent on the temperature in the sol state when the temperature is high, while in the gel state, both G' and G'' are affected by f. In a conventional gel, the gelation

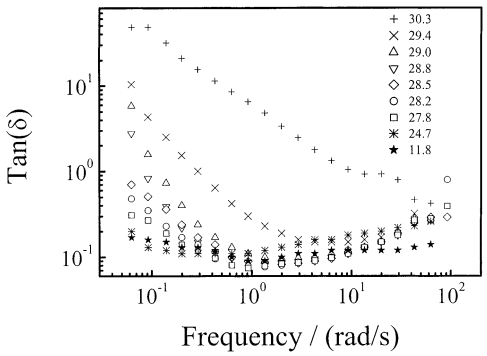

Figure 6. Values of tan(δ) over the entire frequency range, where the microgel concentration is 4.91×10^{-2} g/mL and $\sigma = 1$ Pa.

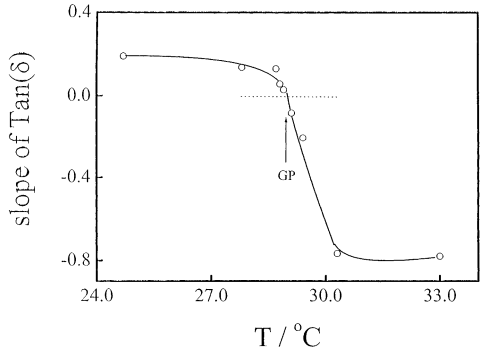

Figure 7. Temperature dependence of the slope of the tan(δ) vs frequency, where the microgel concentration is 4.91×10^{-2} g/mL and $\sigma = 1$ Pa.

corresponds to an increase of the interchain crosslinking and a progressive topologic change from a viscous solution to an elastic gel. In the present case, the gelation involves the formation of close-packed microgel clusters. Note that the size of such clusters increased as the temperature decreased. A lower frequency could probe larger clusters so that the intersection temperature decreases with frequency. A combination of Figures 4 and 5 shows that in the present case the intersection temperature does not correspond to the gelation point, which forced us to look at the method used by Winter et al.[5,27]

Figure 6 shows the shear frequency (f) dependence of the loss tangent tan(δ). Only in a very limited range 0.6−6 rad/s does the slope of log[tan(δ)] vs log(f) change from positive to negative as the temperature increases. In the low-frequency range (<0.6 rad/s), the slope remains negative. The upturn at lower frequencies indicates a "fluidlike" behavior under stress because of the nature of such a hybrid gel network; namely, individual microgels are physically close-packed. Therefore, they could follow the slow oscillation and slide with each other, just like a liquid, if f is sufficiently low. On the other hand, when $f >$ ~6 rad/s, the slope is positive even in the sol state (29 and 29.4 °C), appearing like a "solid". This is because individual swollen microgels (~200 nm) could not move with a high frequency in a concentrated dispersion. The slope change in the limited frequency range (0.6−6 rad/s) provided an estimate of the gelation point at which the slope approaches zero, as shown in Figure 7. Unfortunately, the frequency range at which tan(δ) can be scaled to f was so limited that we could not precisely determine the sol−gel transition point by using the Winter and Chambon method. For the more orderly packed structure, the gel

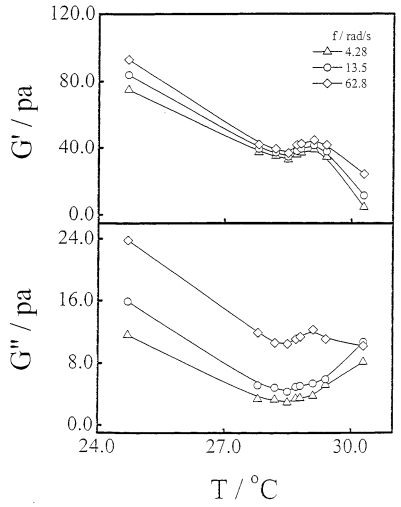

Figure 8. Temperature dependence of the storage moduli (G') and loss moduli (G'') at fixed frequencies, where the microgel concentration is 4.91×10^{-2} g/mL and $\sigma = 1$ Pa.

particles may strongly interact with each other through their dangling chains on the surface of the gel particles. Therefore, both G' and G'' increased within this range for the high-frequency shear.

Figure 8 showed that, on one hand, for a given stress and frequency the storage modulus G' shows an expected decrease when the hybrid gel melts as the temperature increases. On the other hand, there is an unexpected small bump near the melting temperature. Our explanation is as follows. As the temperature increased in the range 25−28 °C, close-packed microgels started to move under the shearing force because the shrinking of individual microgels led to a larger free volume, resulting in the decreases of both G' and G''. Further increase of the temperature in the range 28.5−29 °C reduced the volume fraction of the microgels to such an extent that they became more mobile, resulting in a more orderly packed structure under shear. We may note that the height of the bump depends on the shearing frequency. This is because for the more orderly packed structure the interaction between the microgels via the dangling chains on surface is stronger so that both G' and G'' increase as the shearing frequency in this range. Therefore, both G' and G'' increased slightly in this temperature range. When the temperature was higher than ∼29 °C, the shrinking of individual microgels finally turned the hybrid gel into a dispersion so that both G' and G'' started to decrease again. The temperature at which both G' and G'' reach their corresponding minima (∼28.5 °C) is very close to the sol−gel transition temperatures estimated using the Winter and Chambon method and the flowing test. The temperature dependence of tan(δ) in Figure 9 shows another view of the sol−gel transition near ∼28.5 °C.

Previous studies showed that when a gel network was fully swollen to equilibrium in solvent, G' could be scaled to the equilibrium polymer concentration (C_e), i.e., $G' \propto C_e^{\alpha}$, where α is a scaling exponent.[29−31] This is also true for the hybrid gels studied. Figure 10 shows that α monotonically increases as the temperature. The deviation from the expected value (∼2.25) for gels in a good solvent reflects the decreasing solvent power of water for PNIPAM with increasing temperature. Figure 11 shows the temperature dependence of G' and G'' of the hybrid gels of different concentrations. As expected, the intersection temperature between G' and G'' increases with the concentration because in a more concentrated microgel dispersion, the volume concentration induced sol−gel transition requires less swelling of individual microgels. As discussed before, the intersection temperature varies with the shearing stress and frequency. Therefore, we could use the turning point in the temperature dependence of tan(δ) to estimate the sol−gel temperature, as shown in Figure 12. In this way, we avoid the difficulty of using the Winter and Chambon method because the scaling of log[tan(δ)] vs log(f) was only in a limited frequency range in the present case.

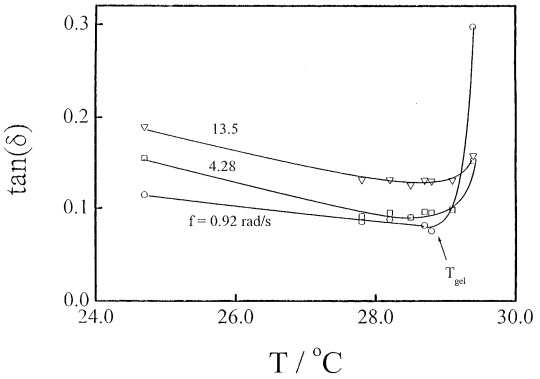

Figure 9. Temperature dependence of the tan(δ) at fixed frequencies, where the microgel concentration is 4.91×10^{-2} g/mL and $\sigma = 1$ Pa.

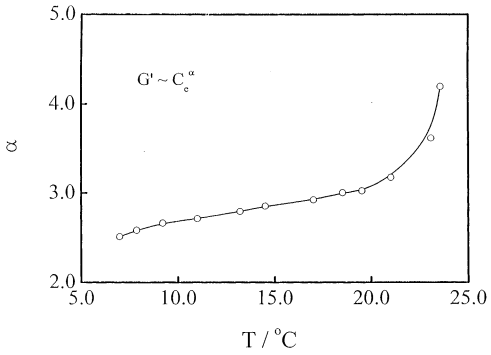

Figure 10. Temperature dependence of the slope of the ln(G') vs ln(C_e), where $f = 1$ Hz and $\sigma = 1$ Pa. C_e was calculated from the temperature dependence of the hydrodynamic volume of microgels.

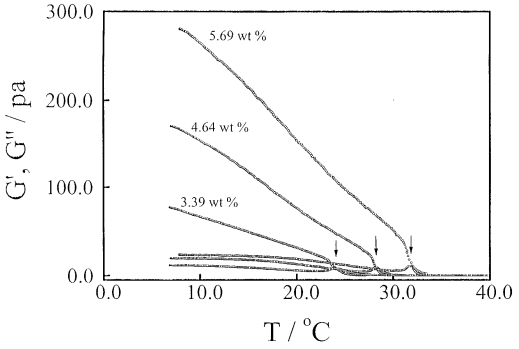

Figure 11. Temperature dependence of the dynamic moduli (G' and G'') for the PNIPAM hybrid gel systems, where the microgel concentration is 3.39×10^{-2}, 4.64×10^{-2}, and 5.69×10^{-2} g/mL, $\sigma = 1$ Pa, and $f = 1$ Hz.

Conclusion

The close-packing of billions of spherical poly(*N*-isopropylacrylamide) microgels in a concentrated dis-

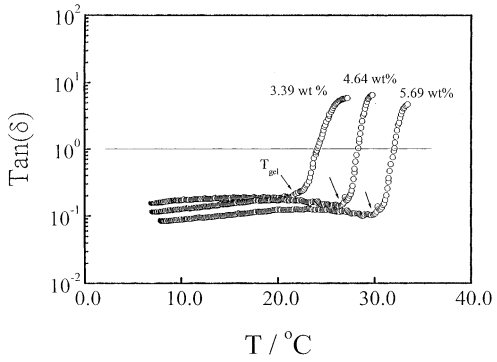

Figure 12. Temperature dependence of tan δ (tan $\delta = G''/G'$) for the gels system, where the microgel concentrations is 3.39×10^{-2}, 4.64×10^{-2}, and 5.69×10^{-2} g/mL, $\sigma = 1$ Pa, and $f = 1$ Hz.

persion can lead to a sol−gel transition to form an elastic hybrid gel. The viscoelastic study of such hybrid gels showed that the intersecting temperature between the storage and loss modulus (G' and G'') depended on both the shearing frequency (f) and shearing stress (σ). Therefore, for the hydrogels, such an intersecting point cannot be used to estimate the sol−gel transition temperature. On the other hand, for a given shear stress, the scaling of the loss tangent tan(δ) to shearing frequency (f) appears only in a very limited range so that we were not able to accurately determine the sol−gel transition temperature from the point at which tan(δ) was independent of f, indicating that the behavior of the hybrid gels was quite different than predicted by Winter et al.[27] However, our results showed that during the sol−gel transition the slope of the temperature dependence of tan(δ) changes from positive to negative. The turning point corresponds well to the sol−gel transition temperature observed in the flow test. At the sol−gel transition temperature, tan(δ) is independent of the shearing frequency and $\delta = n\pi/2$ with $n = 0.06$, indicating that the hybrid gels are fairly elastic. As expected, the sol−gel transition temperature increases with the microgel concentration. The sol−gel transition of the hybrid gel is much faster than that of a bulk PNIPAM hydrogel with a similar solid content. This leads to potential biomedical applications which will be reported in a coming paper.

Acknowledgment. The financial support of the Special Funds for Major State Basic Research Projects (G1999064800), the CAS Bai Ren Project, the NSFC projector (29974027), and the HKSAR Earmarked RGC Grants (CUHK, 2160135) is gratefully acknowledged.

References and Notes

(1) Brinker, C. J.; Scherer, G. W. In *Sol−Gel Science*; Academic Press: San Diego, 1990.
(2) Hench, L. L., Ulrich, D. R., Eds.; In *Science of Ceramic Chemical Processing*; Wiley: New York, 1986.
(3) Larson, R. G. In *The Structure and Rheology of Complex Fluids*; Oxford University Press: New York, 1999; Chapter 5.
(4) Lapasin, R.; Pricl, S. In *Progress and Trends in Rheology V*; Emri, I., Cvelbar, R., Eds.; Springer: Berlin, 1998.
(5) Winter, H. H. In *Encyclopedia of Polymer Science and Engineering*; John Wiley & Sons: New York, 1989.
(6) Almdal, K.; Dyre, J.; Hvidt, S.; Kramer, O. *Polym. Gels Networks* **1993**, *1*, 5−17.
(7) Hench, L. L.; West, J. K. *Chem. Rev.* **1990**, *90*, 33−72.
(8) Gabriel, A. O.; Riedel, R. *Angew. Chem., Int. Ed. Engl.* **1997**, *36*, 384−386.
(9) Gabriel, A. O.; Riedel, R.; Storck, S.; Maier, W. F. *Appl. Organomet. Chem.* **1997**, *11*, 833−841.
(10) Clark, A. H.; Ross-Murphy, S. B. *Adv. Polym. Sci.* **1987**, *83*, 58.
(11) Grisel, M.; Muller, G. *Macromolecules* **1998**, *31*, 4277−4281.
(12) Hone, J. H. E.; Howe, A. M.; Cosgrove, T. *Macromolecules* **2000**, *33*, 1199−1205.
(13) Balan, C.; Volger, K. W.; Kroke, E.; Riedel, R. *Macromolecules* **2000**, *33*, 3404−3408.
(14) Daoud, M. *Macromolecules* **2000**, *33*, 3019−3022.
(15) Yoon, P. J.; Han, C. D. *Macromolecules* **2000**, *33*, 2171−2183.
(16) Tanaka, F. *Macromolecules* **1998**, *31*, 384−393.
(17) Matricardi, P.; Dentini, M.; Crescenzi, V. *Macromolecules* **1993**, *26*, 4386−4387.
(18) Anseth, K. S.; Anderson, K. J.; Bowman, C. N. *Macromol. Chem. Phys.* **1996**, *197*, 833−848.
(19) Zhao, Y.; Zhang, G. Z.; Wu, C. *Macromolecules* **2001**, *34*, 7804−7808.
(20) Wu, C.; Zhou, S. Q. *J. Polym. Sci., Polym. Phys. Ed.* **1996**, *34*, 1597−1604.
(21) Chu, B. *Laser Light Scattering*, 2nd ed.; Academic Press: New York, 1991.
(22) Berne, B.; Pecora, R. *Dynamic Light Scattering*; Plenum Press: New York, 1976.
(23) Wu, C.; Zhou, S. Q. *Macromolecules* **1995**, *28*, 8381−8387.
(24) Sacks, M. D.; Sheu, R. S. *J. Non-Cryst. Solids* **1987**, *92*, 383−396.
(25) Tung, C. Y. M.; Dynes, P. J. *J. Appl. Polym. Sci.* **1982**, *27*, 569.
(26) Macosko, C. W. *Rheology: Principles, Measurements, and Applications*; VCH Publishers: New York, 1994.
(27) Winter, H. H.; Chambon, F. J. *J. Rheol.* **1986**, *30*, 367−382; **1987**, *31*, 683−697.
(28) Power, D. J.; Rodd, A. B.; Paterson, L.; Boger, D. V. *J. Rheol.* **1998**, *42*, 1021−1037.
(29) de Gennes, P. G. *Scaling Concepts in Polymer Physics*; Cornell University Press: Ithaca, NY, 1979; Chapter 5.
(30) Hild, G. *Prog. Polym. Sci.* **1998**, *23*, 1019−1149.
(31) Gnanou, Y.; Hild, G.; Rempp, P. *Macromolecules* **1987**, *20*, 123.

MA020919Y